

Standard Transport Channels of X-ray Beamlines at SPring-8

Shunji Goto,^{a*} Makina Yabashi,^a Haruhiko Ohashi,^a Hiroaki Kimura,^a Kunikazu Takeshita,^a Tomoya Uruga,^a Tetsuro Mochizuki,^a Yoshiki Kohmura,^b Masanori Kuroda,^b Masaki Yamamoto,^b Yukito Furukawa,^b Nobuo Kamiya^b and Tetsuya Ishikawa^b

^aJapan Synchrotron Radiation Research Institute, SPring-8, Kamigori 678-12, Japan, and

^bJAERI-RIKEN SPring-8 Project Team, SPring-8, Kamigori 678-12, Japan.

E-mail: sgoto@spring8.or.jp

(Received 10 October 1997; accepted 23 December 1997)

SPring-8 is constructing most of its beamlines using a combination of standardized components. The structures of the beamlines are also standardized according to the light-source characteristics. Specifications of components as well as the unified method of assembly and alignment are described.

Keywords: beamline; transport channel; standard components.

1. Introduction

Towards the dedicated user operation from October 1997, SPring-8 is now finalizing more than ten beamlines. At least two or three beamlines are planned to be added every year. To manage simultaneous and/or continual construction of many beamlines, it is important to standardize the beamline components. In view of this, the SPring-8 project team have commenced the standardization of components including insertion devices (Hara *et al.*, 1998), front ends (Sakurai *et al.*, 1998) and also components of the transport channels which are part of the beamlines outside the accelerator shielding wall.

The underlying principle of standardization for beamline transport-channel components reported by Ishikawa (1996) is that any components used for the same purpose should have similar mechanical structures. A detailed specification of each component was fixed (Ishikawa, 1997; Goto, Mochizuki *et al.*, 1997) according to this principle. An actual design study was made in collaboration with the manufacturers of the components.

As for the X-ray beamlines constructed in the first phase, layouts of the transport channels were also standardized. In parallel, simpler methods of assembling standard components into beamline transport channels were surveyed (Goto, Yabashi *et al.*, 1997) to facilitate simultaneous construction of many beamlines, and also to reduce the period of construction.

This report will show briefly how the standard transport channels were constructed at SPring-8. Some details of the beamline transport channels are given, including specifications of components as well as the procedure for assembly and alignment.

2. Standard components and layouts of transport channels

Several key components for X-ray beamlines, listed in Table 1, were selected from the viewpoints of radiation

Table 1

List of transport channel components and flange-to-flange distances.

Components	Flange-to-flange distance (mm)		
	ICF70 for undulator	ICF114 for bending magnet	ICF152 for bending magnet
Bellows	200	300	300
Be window			
Downstream shutter	400	400	400
γ -stopper	600	600	600
Helium chamber for Be window			
Post for standard component (PST1)			
Post for vacuum tube (PST2)			
Pumping unit			
Pumping port	300	300	300
Gauge port	200	200	200
Slit for monochromatic X-rays	280	360	380
Vacuum tube			
View port (screen monitor)	200	350	350
Water-cooled slit	None	500	500
X-ray stopper			

shielding (Asano, 1998), beam monitoring, beam shaping and vacuum considerations. They are standardized according to the source and optical characteristics of the beamlines. Standard vacuum ducts with conflat flanges of diameter 70 mm (114 mm or 152 mm) were adopted as the beam ducts of these components for undulator (bending-magnet) beamlines, since the inner diameters of the ducts are large enough for typical beam sizes. For each of them, the basic specifications were fixed as shown in Table 2 from mechanical and safety considerations. All vacuum components are high-vacuum compatible with a designed pressure down to at least 10^{-4} Pa attainable by turbo-molecular pumps. The flange-to-flange distance of each vacuum component listed in Table 1 was fixed before the detailed design was finalized, since this enabled independent design

Table 2
Basic specifications of main components.

Component	ICF70 for undulator	Flange type ICF114 for BM	ICF152 for BM
Beryllium window			
Be thickness (mm)	0.2	0.2	0.2
Aperture size (mm)	10 (diameter)	15 × 40	15 × 60
Downstream shutter			
Pb thickness (mm)	94	94	94
γ -stopper			
Pb thickness (mm)	350	350	350
Pb area [H (mm) × W (mm)]	325 × 300	325 × 300	325 × 300
Screen monitor			
Screen size (mm)	20 × 20	20 × 100	20 × 100
Slit for monochromatic X-rays			
Resolution ($\mu\text{m step}^{-1}$)	1	1	1
Stroke (horizontal) (mm)	−5 → +5	−5 → +35	−5 → +35
Stroke (vertical) (mm)	−5 → +5	−5 → +5	−5 → +5
Ta blade thickness (mm)	2	2	2
Water-cooled slit			
Resolution ($\mu\text{m step}^{-1}$)	None	0.5	0.5
Stroke (horizontal) (mm)	None	−5 → +35	−5 → +35
Stroke (vertical) (mm)	None	−20 → +20	−20 → +20
Cu and Ta blade thicknesses (mm)	None	10 and 5	10 and 5
X-ray stopper			
Pb thickness (mm)	100	100	100
Pb area [H (mm) × W (mm)]	300 × 300	300 × 300	300 × 300

Table 3
Optics layout for standard hard X-ray bending-magnet beamlines showing distances from the source point.

B: bent mirror; V: vertical reflection.

Bending magnet beamline	BL01B1	BL02B1	BL04B1 (white)
Be window (front-end)	27.3 m	26.1 m	30.8 m
Collimator mirror	32.9 m (B, V)	28.7 m (B, V)	None
Monochromator	35.9 m	31.7 m	None
Refocusing mirror	42.1 m (B, V)	37.9 m (B, V)	None
Be window	46.5 m	42.3 m	37.3 m

processes of the individual components and the total beamline.

A design study of the total beamlines was commenced by locating key optical components, such as total reflection mirrors (Uruga *et al.*, 1998), and double-crystal monochromators (Ishikawa, 1998), at appropriate positions, which were determined from various optical considerations and the geometrical limitation of the building. For undulator X-ray beamlines, a double-crystal monochromator followed by optional total reflection mirror(s) was set up as a standard structure. There are five transport channels within this structure. On the other hand, the first collimating mirror, and a double-crystal monochromator, followed by the second refocusing mirror, were set up as a standard structure for the transport channel of a bending-magnet beamline. Although the structure was standardized according to the type of radiation source and optics, fine adjustment of the component position was needed to reflect the differences in the building structure. The final position parameters of the key optical components are listed in Tables 3 and 4. After locating the optical components, the positions of other components were fixed

according to the general layout as well as to the unification principles set up by the SPring-8 beamline construction group, some of which are shown below as examples.

(i) After the monochromator, a γ -ray stopper, a screen monitor and a downstream shutter should be located in this order.

(ii) The transport channel should be divided into several vacuum sections by gate valves. Each section should be equipped with at least one pumping unit at an adequate position to keep the vacuum pressure less than 10^{-3} Pa. An appendage turbo-molecular pump may be added to a large-volume component such as the monochromator.

(iii) The first vacuum section of the transport channel has only the pumping unit and vacuum-maintenance-free components in order to protect the front-end beryllium window.

The typical structure of a beamline transport channel has been presented by Ishikawa (1998) and in the *SPring-8 Beamline Handbook 1997* (Japan Synchrotron Radiation Research Institute, 1997).

3. Deflection stage and elevation stage for standard bending-magnet beamlines

As a standard structure of bending-magnet beamlines, we adopted collimating mirror–monochromator–refocusing mirror optics. These optics have multiple roles to improve the energy resolution, to reject higher harmonics, and to deliver a higher flux density at a sample position. Fig. 1 shows the glancing angles and squared reflectivities resulting from reflections of two mirrors as functions of the fundamental photon energy which gives the damping ratio of the third harmonics as 10^{-4} , 10^{-5} and 10^{-6} . A surface

Table 4

Optics layout for standard hard X-ray undulator beamlines showing distances from the source point.

B: bent mirror; P: plane mirror; V: vertical reflection; H: horizontal reflection; D: double mirror.

Undulator beamline	BL09XU	BL10XU	BL39XU	BL41XU	BL47XU
Be window (front end)	33.9 m	33.9 m	33.9 m	33.9 m	33.9 m
Monochromator	37.6 m	37.6 m	36.0 m	35.9 m	35.9 m
Mirror (first)	None	45.7 m (P, V, D)	44.0 m (P, H)	39.5 m (B, V)	None
Mirror (second)	None	None	None	44.0 m (B, H)	None
Be window	47.1 m	49.1 m	46.2 m	49.8 m	44.2 m

roughness of 0.5 nm (r.m.s.) is assumed for the reflectivity calculation. Between 10 and 30 keV, the glancing angle should be set at 2–7 mrad to obtain an adequate damping ratio of higher harmonics, with resulting deflection angles of 4–14 mrad.

To align the centre of the components to the beam axis, which varies with the deflection angle of the total reflection mirror, deflection and elevation stages were devised as standard components for bending-magnet X-ray beamlines. The maximum deflection angle is designed to be 20 mrad. Fig. 2 shows these stages schematically. The deflection stage supports the monochromator, the γ -ray stopper and other components placed between the two mirrors, and the

elevation stage lifts the refocusing mirror and downstream components. The total weight of components to be mounted on the deflection stage exceeds 3000 kg. Since a big vacuum chamber of the standard monochromator is mounted on the stage, the maximum stage height from the floor level is limited to 475 mm when the deflection angle is set at zero. Although the ideal position of the pivot of deflection would agree with the rotation axis of the collimator mirror, limited space around the mirror chamber

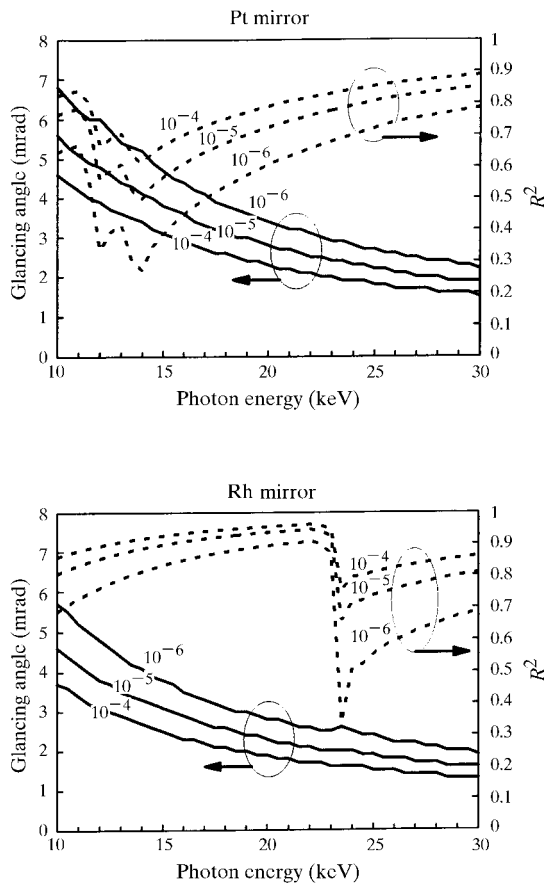


Figure 1

Glancing angle and squared reflectivity (reflection from two mirrors) as a function of fundamental photon energy to obtain third-harmonics rejection ratios of 10⁻⁴, 10⁻⁵ and 10⁻⁶. A surface roughness of 0.5 nm (r.m.s.) is assumed for reflectivity calculation.

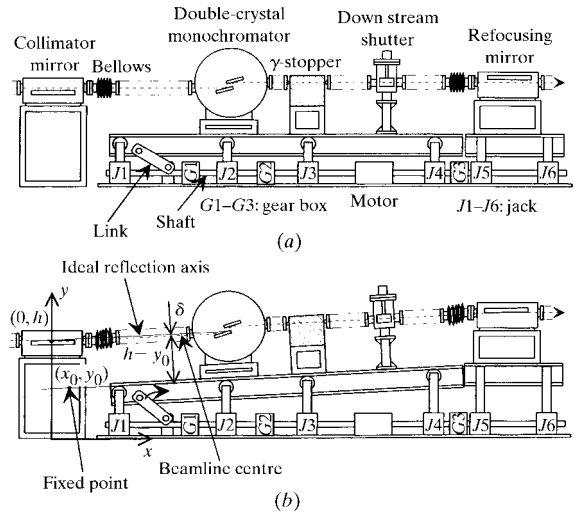


Figure 2

Schematic diagram of (a) the deflection and (b) the elevation stages for SPring-8 standard bending-magnet beamlines.

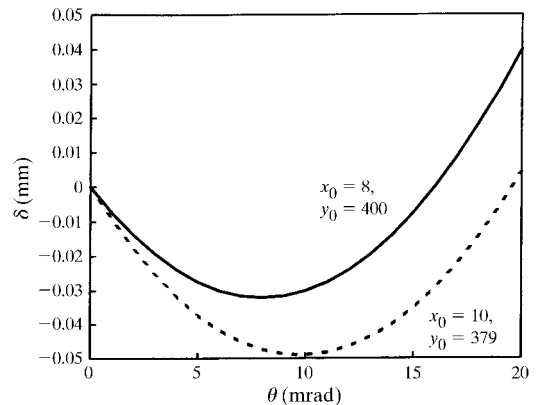


Figure 3

Deviation, δ , of beamline component centre from the ideal beam axis reflected by the collimator mirror as a function of deflection angle.

prevents this. Instead, the deflection stage is supported by a series of jacks with rollers on the head. A link mechanism is used to avoid a shift upstream due to the inclination. The inclination angle of the deflection stage, as well as the height of the elevation stage, are mechanically linked by using driving shafts connected through appropriate gear boxes. Using this mechanism, the deviation, δ , of the beamline component centre from the ideal beam axis reflected by the collimating mirror is given by

$$\delta = (h - y_0)(1 - \cos \theta) - x_0 \sin \theta, \quad (1)$$

where h is the incident beam height to the collimator mirror, θ is the deflection angle, and x_0, y_0 are the coordinates at a fixed position of extension on the rollers (Fig. 2). To minimize $\int_0^{\theta_{\max}} \delta^2 d\theta$ for given h and y_0 , we obtain

$$x_0 = (h - y_0) \frac{\int_0^{\theta_{\max}} (1 - \cos \theta) \sin \theta d\theta}{\int_0^{\theta_{\max}} \sin^2 \theta d\theta}. \quad (2)$$

Fig. 3 shows the calculated deviation, δ , as a function of the deflection angle. For example, we obtain $x_0 = 8$ mm and maximum $\delta = 0.04$ mm for $\theta_{\max} = 20$ mrad, $h = 1400$ mm, and $y_0 = 400$ mm. Actually, we used the values $x_0 = 10$ mm and $y_0 = 379$ mm due to a limitation of the mechanical design. In this case, the maximum deviation, δ , is 0.05 mm, which is acceptable for beamline utilization.

4. Alignment

Since vacuum ducts for each transport channel have a large enough diameter for the beam to pass through, a major restriction of alignment comes from the allowance of the standard bellows. The permissible error for alignment was set to be ± 1 mm along the beamline and ± 0.5 mm perpendicular to the beam axis. These errors are well absorbed by the standard bellows.

The first step of the alignment was to draw a reference line of the floor which is a projection of the beam axis. Reference points corresponding to each component were marked on the line. Alignment targets were made by fitting points with 1 mm-diameter holes at the centre of conflat flanges. A set of alignment tools which are commonly used for standard components (Goto, Yabashi *et al.*, 1997) was prepared. The targets were attached to both sides of the component flanges and plummets were suspended from the

target holes. Horizontal positions of the components were adjusted by pushing adjusting screws so that the plummets agreed with the reference line and points. Vertical positions were adjusted by using stud bolts, monitored by two surveyor's levels set at designed levels. This method of alignment was applied even when the alignment was made along an inclined beam axis such as downstream of the vertically deflecting mirror by setting the surveyor's levels at calculated levels. Similar methods are also used to align the monochromators, mirror chambers and other optical components.

5. Concluding remarks

Most X-ray transport channels at SPring-8 are composed of standardized components. The structures of the transport channels are also standardized according to the source characteristics. By adopting the alignment method described in this report, X-rays were led to the approximate centre of the Be window at the end of the beamlines.

References

- Asano, Y. (1998). *J. Synchrotron Rad.* **5**, 615–617.
- Goto, S., Mochizuki, T., Kimura, H., Ohashi, H., Takeshita, K. & Ishikawa, T. (1997). *SPring-8 Annual Report 1996*, pp. 230–232. SPring-8, Kamigori 678-12, Japan.
- Goto, S., Yabashi, M., Takeshita, K., Uruga, T., Furukawa, Y. & Ishikawa, T. (1997). *SPring-8 Annual Report 1996*, pp. 233–234. SPring-8, Kamigori 678-12, Japan.
- Hara, T., Tanaka, T., Tanabe, T., Marechal, X.-M., Okada, S. & Kitamura, H. (1998). *J. Synchrotron Rad.* **5**, 403–405.
- Ishikawa, T. (1996). *SPring-8 Annual Report 1995*, pp. 38–43. SPring-8, Kamigori 678-12, Japan.
- Ishikawa, T. (1997). *SPring-8 Annual Report 1996*, pp. 30–32. SPring-8, Kamigori 678-12, Japan.
- Ishikawa, T. (1998). *SRI'97 Meeting*, Abstract 5M02.
- Japan Synchrotron Radiation Research Institute (1997). *SPring-8 Beamline Handbook*, Version 1.1. SPring-8, Kamigori 678-12, Japan.
- Sakurai, Y., Oura, M., Takahashi, S., Hayashi, Y., Aoyagi, H., Shiwaku, H., Kudo, T., Mochizuki, T., Oikawa, Y., Takahashi, M., Yoshii, K. & Kitamura, H. (1998). *J. Synchrotron Rad.* **5**, 1195–1198.
- Uruga, T., Ohtomo, K. & Ishikawa, T. (1998). *J. Synchrotron Rad.* Submitted.